RESIDUAL STRESSES IN NON-SYMMETRICAL CARBON/EPOXY LAMINATES

S. Wijskamp, R. Akkerman and E.A.D. Lamers

University of Twente, Faculty of Engineering Technology, Composites Group
P.O. Box 217, 7500 AE Enschede, The Netherlands
email: s.wijskamp@ctw.utwente.nl

ABSTRACT

The curvature of unsymmetrical [0/90] laminates moulded from AS4/8552 uni-directional tape has been measured. A linear thermoelastic approach has been applied to predict the related residual stress state before demoulding, giving an estimate of the stress induced by polymerisation strain. The results from the linear approach are confirmed by a viscoelastic finite element model including the cure conversion and related change in viscosity. It is concluded that the curvature measurement of unsymmetrical laminates is an accurate method for the prediction of the transverse residual stress, making it suitable as a benchmark for complex stress modelling.

keyterms: residual stress, thermoset, cure shrinkage, viscoelastic, finite elements.

1 INTRODUCTION

Polymer composite products are increasingly applied in demanding structures in, for example, the aerospace and the aeronautical industry. The narrow tolerances on the product geometry require the control of undesirable post-mould distortions such as warpage and spring-forward. The key to this control is the understanding of the internal stresses that build up during the moulding cycle and residual stresses that reside afterwards. These stresses are caused by material anisotropy, chemical and thermal shrinkage, the lay-up of the laminate, etc., or they are induced by the moulding process. The prediction of the internal stresses and the resulting product distortions contributes to a 'first-time-right' design of the tooling and in the reduction of scrap material.

In this paper, the residual stresses of 8552/AS4 laminates are considered. The accurately determined curvature of non-symmetric [0/90]] laminates is used as a measure for the residual stress profile before release from the tool. At first, the stresses are predicted with a linear model including thermal and chemical shrinkage [1]. Secondly, the experimental results and the results from the linear model are compared to a more complex stress analysis performed with the Finite Element (FE) method, applying a viscoelastic material model.

2 EXPERIMENTAL WORK

Unsymmetrical $[0_4/90_4]$ laminates were cured on a flat composite tool in an autoclave oven according to the temperature cycle as shown in figure 1. The cycle consisted of a ramp-up at 2 °C/s from room temperature to the cure temperature of 180 °C, a dwell period of 2 hours and finally cooling to room temperature at 4 °C/s.

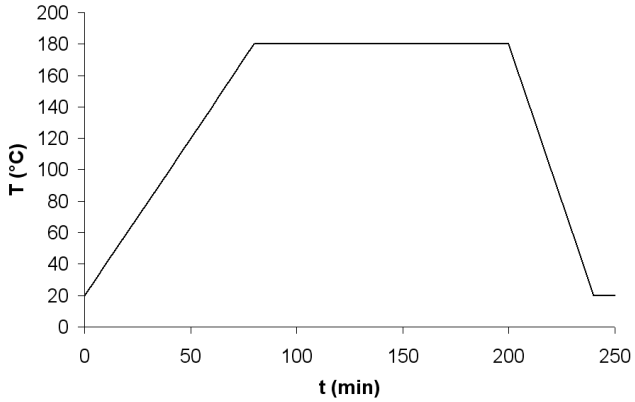

figure 1. Autoclave temperature profile for the curing of the [0_4/90_4] AS4/8552 laminates

The cured laminates with in-plane dimensions of 500×100 mm^2 and a thickness of 1.55 mm showed a saddle-shaped geometry with curvatures $\kappa_x = -\kappa_y$. The laminates were cut to specimens of 100×10 mm^2 using a water-cooled diamond saw. The dimensions were chosen after a numerical analysis of the geometrical non-linearity that occurs with curved plates, employing a minimisation of potential energy method [2,3]. Presumably, the saddle-shape of the specimens is stable and hence not sensitive to minor differences in width or length.

The sawed pieces were cleaned, weighed and placed into a vacuum oven at 80 °C for intensive drying. The desiccation was followed through weighing until an asymptotic value of the mass had been reached.

The shape of the curved specimens was scanned with a co-ordinate measurement device. This device consists of two stepper motor controlled arms for in-plane (*x*- and *y*-directions) movement and a rigidly mounted NCDT laser reflector for non-contact scanning of the specimen's surface in the *z*-direction normal to the horizontal plane. The curvature measurements were performed with a step size of 1.25 mm over 95 mm of the 100 mm length of the specimens, giving 77 data points. The co-ordinates of the scanned surface were then fed into a curve fitting routine. A second order polynomial $z = ax^2 + bx + c$ was fitted, after which the curvature could be derived according to:

$$\kappa_x = -\frac{\partial^2 z}{\partial x^2} = -2a \tag{1}$$

The specimens were shortly heated-up to their presumed stress-free temperature to reverse possible relaxation of internal stresses. This stress-free temperature was assumed to be equal to the curing temperature of 180 °C, although Gigliotti et al. [4] measure a slightly higher temperature of approximately 190 °C attributed to non-thermoelastic strain due to chemical shrinkage, stress relaxation and interaction with the tool. The average curvature of the six specimens after reheating was measured to be 3.14 m^{-1} with a standard deviation of 0.06 m^{-1}.

3 ANALYTICAL APPROACH

The classical laminate theory

The constitutive behaviour of composite plates is described by the classical laminate theory (CLT) [5], which relates the in-plane force and moment resultants per unit width, respectively $\{N\}$ and $\{M\}$, to the midplane strains and curvatures $\{\varepsilon^0\}$ and $\{\kappa\}$:

$$\begin{Bmatrix} N \\ M \end{Bmatrix} = \begin{bmatrix} A & B \\ B & D \end{bmatrix} \begin{Bmatrix} \varepsilon^0 \\ \kappa \end{Bmatrix} \tag{2}$$

where

$$\left(A_{ij},\ B_{ij}, D_{ij}\right)=\sum_{k=1}^{K}\int_{h_B^k}^{h_T^k}(1, z, z^2)Q_{ij}^k dz \qquad i, j = 1, 2, 6 \tag{3}$$

Here, Q_{ij}^k is the reduced stiffness matrix of the k^{th} ply transformed to the global laminate co-ordinate system, h_B^k and h_T^k are the bottom and top co-ordinate of the k^{th} ply, respectively, z is the thickness co-ordinate and K denotes the total number of plies. The inverse form of (2) is defined as

$$\begin{Bmatrix}\varepsilon^0\\ \kappa\end{Bmatrix}=\begin{bmatrix}a & b\\ h & d\end{bmatrix}\begin{Bmatrix}N\\ M\end{Bmatrix},\ \begin{bmatrix}a & b\\ h & d\end{bmatrix}=\begin{bmatrix}A & B\\ B & D\end{bmatrix}^{-1} \tag{4}$$

Relation between stress before release and curvature after release

The curvature and midplane strain of the cured laminate are directly related to the internal stress state at the end of the curing cycle. Consider the anti-symmetric laminate before it is released from the tool. The boundary conditions will be similar in all in-plane directions during the production process. Assume planar isotropy for these possible tractions or prescribed deformations. Then in both unidirectional sublaminates the stresses in the fibre direction σ_1 will be equal and homogeneous. The same holds for the transverse normal stresses σ_2. The stress profile through the thickness (in the *xz*-plane) is depicted in figure 2.

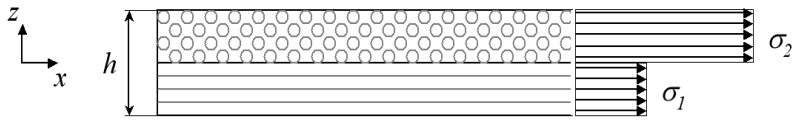

figure 2. Normal stress profile in a [0/90] laminate before release from the tool

The internal force and moment resultant are obtained according to

$$\begin{aligned} N_x = N_y &= \int_{-h/2}^{h/2}\sigma(z)dz = \frac{h}{2}(\sigma_1+\sigma_2)\\ M_x = -M_y &= \int_{-h/2}^{h/2}\sigma(z)z dz = \frac{h^2}{8}(\sigma_1-\sigma_2)\end{aligned} \tag{5^{a,b}}$$

where h is the thickness of the laminate. The midplane strain and curvature induced by these internal forces and moments are expressed in terms of the normal stresses by substituting (5^{a,b}) in (4)

$$\begin{aligned}\varepsilon_x^0 = \varepsilon_y^0 &= \left(-\frac{h}{2}(a_{11}+a_{12})-\frac{h^2}{8}b_{11}\right)\sigma_1+\left(-\frac{h}{2}(a_{11}+a_{12})+\frac{h^2}{8}b_{11}\right)\sigma_2\\ \kappa_x = \kappa_y &= \left(\frac{h^2}{8}(d_{12}-d_{11})-\frac{h}{2}b_{11}\right)\sigma_1+\left(\frac{h^2}{8}(d_{11}-d_{12})-\frac{h}{2}b_{11}\right)\sigma_2\end{aligned} \tag{6^{a,b}}$$

recognising that the compliance matrix of a [0/90] laminate contains the following coefficients:

$$\begin{bmatrix} a & b \\ b & d \end{bmatrix} = \begin{bmatrix} a_{11} & a_{12} & 0 & b_{11} & 0 & 0 \\ a_{12} & a_{11} & 0 & 0 & -b_{11} & 0 \\ 0 & 0 & a_{11} & 0 & 0 & 0 \\ b_{11} & 0 & 0 & d_{11} & d_{12} & 0 \\ 0 & -b_{11} & 0 & d_{12} & a_{11} & 0 \\ 0 & 0 & 0 & 0 & 0 & d_{66} \end{bmatrix} \tag{7}$$

Having reasonable confidence in the correctness of the compliance matrix, σ_1 and σ_2 can be solved directly from the experimentally obtainable midplane ε^0 and κ. Here, this approach is not applicable as the midplane strain was not measured. However, the stresses can be estimated:

$$\begin{Bmatrix} \sigma_1 \\ \sigma_2 \end{Bmatrix} = [Q^1] \begin{Bmatrix} \varepsilon_{mech} - \alpha_1 \Delta T - \psi_1 \\ \varepsilon_{mech} - \alpha_2 \Delta T - \psi_2 \end{Bmatrix} = [Q^1] \begin{Bmatrix} -\alpha_1 \Delta T - \psi_1 \\ -\alpha_2 \Delta T - \psi_2 \end{Bmatrix} \tag{8}$$

where $\alpha_{1,2}$ and $\psi_{1,2}$ are the coefficients of thermal expansion and chemical shrinkage in principal directions, respectively. Here, the mechanical strain ε_{mech} is equal to zero as the laminate is assumed to be restricted by the presumably rigid tool. It is assumed that the resin has fully cured upon the start of cooling, so the thermal stresses are effectively growing from T_{sf} to room temperature. The contribution of the chemical shrinkage is less transparent; the amount of shrinkage after the vitrification point, often assumed as the point where the resin becomes elastic and is able to pick-up stress, is generally not available and requires extensive chemorheological characterisation. Nevertheless, the total chemical shrinkage is presumed as stress-inducing for a first guess. The coefficients $\psi_{1,2}$ are derived with micromechanics rules for uni-directional (UD) plies [6]:

$$\{\psi\} = \begin{Bmatrix} \psi_1 \\ \psi_2 \\ \psi_3 \end{Bmatrix} = \begin{Bmatrix} \dfrac{V_m E_m}{V_f E_f + V_m E_m} \\ (1+\nu_m) V_m - \dfrac{V_m E_m (V_f \nu_f + V_m \nu_m)}{V_f E_f + V_m E_m} \\ (1+\nu_m) V_m - \dfrac{V_m E_m (V_f \nu_f + V_m \nu_m)}{V_f E_f + V_m E_m} \end{Bmatrix} \varepsilon_{cure}^{resin} \tag{9}$$

where V_m and V_f are the volume fractions, E_m and E_f are the stiffnesses, ν_m and ν_f are the Poisson's ratios of matrix and fibre, respectively and $\varepsilon_{cure}^{resin}$ represents the chemical shrinkage of the matrix.

Numerical evaluation

The elastic and thermal properties of AS4/8552 UD tape, the computed coefficients of chemical shrinkage and the required coefficients of the compliance matrix are shown in table 1.

property	unit	property	unit	property	unit
E_1	135 GPa	E_f	220 GPa	a_{11}	20.412 mm/MN
E_2	9.6 GPa	ν_f	0.27	a_{12}	-0.8131 mm/MN
G_{12}	5.5 GPa	E_m	3.6 GPa	b_{11}	-34.26 MN^{-1}
ν_{12}	0.3	ν_m	0.37	d_{11}	102.0 $(MN\ mm)^{-1}$
α_1	$2.8 \cdot 10^{-7}$ °C^{-1}	V_f	60%	d_{12}	-4.061 $(MN\ mm)^{-1}$
α_2	$2.8 \cdot 10^{-5}$ °C^{-1}	ψ_1	$6.8 \cdot 10^{-5}$		
$\varepsilon_{resin}^{cure}$	$6.2 \cdot 10^{-3}$	ψ_2	$3.4 \cdot 10^{-3}$		

table 2. Thermal and elastic properties of AS4/8552 unidirectional ply and its constituents

The curvature is calculated as $\kappa_x = -\kappa_y = 4.3\ m^{-1}$, the midplane strain as $\varepsilon_x^0 = \varepsilon_y^0 = 2.1 \cdot 10^{-3}$. Obviously, the computed curvature overestimates the measured curvature of 3.1 m^{-1}. The contribution of thermal stresses to the curvature of unsymmetrical laminates has been established by Eijpe [7]. As argued above, the amount of chemical shrinkage that actually induces stress is questionable. Reducing this amount, which was assumed to be maximal, to 40 % leads to agreement with the experimentally obtained curvature. Figures 3 and 4 respectively show the initially predicted and corrected curvatures split up in a thermally and chemically induced part, and the stresses calculated accordingly.

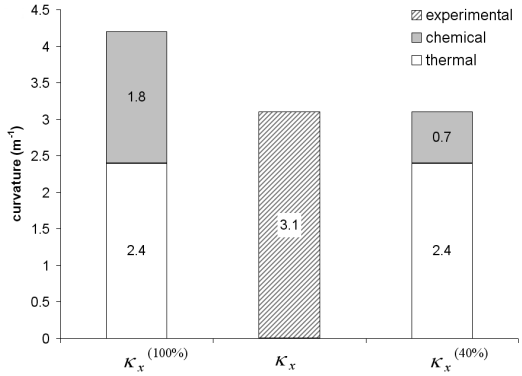

figure3. Initially predicted, measured and adjusted curvature

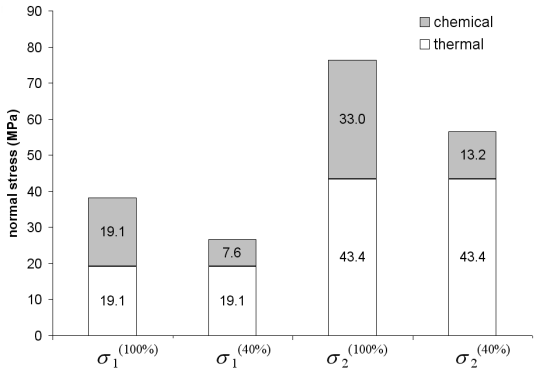

figure 4. Initially predicted and adjusted normal stresses before release

Evaluating (6^b) numerically confirms that the curvature is practically a direct measure for the transverse stress σ_2:

$$\kappa_x = -5.3 \cdot 10^{-3} \sigma_1 + 58.4 \cdot 10^{-3} \sigma_2 \qquad (10^{a,b})$$

The contribution of the longitudinal stress σ_1 to the curvature appears to be negligible for this material, which complicates the validation of the prediction of this stress. Nevertheless, it may be well assumed that the longitudinal stress is induced by the same effects – the thermal and chemical contraction of the resin – as the transverse stress, neglecting the possible stress due to the near-zero thermal expansion of the composite tool.

4 FINITE ELEMENT SIMULATIONS

In the recent years, a number of finite element (FE) based models for the computation of stresses and deformations of thermoset composites has been proposed, see the work by Johnston et al. [8]. In general, the models follow the cure conversion and describe the constitutive behaviour as a function of this conversion. Here, the work by Wiersma et al. [9] on spring-forward of UD

composite L-shapes is extended for the computation of the residual stresses in AS4/8552 unsymmetrical laminates.

Constitutive modelling
Consider a UD ply consisting of a viscoelastic matrix and elastic fibres. The two constituents are modelled as a Maxwell element and a spring, respectively:

$$\boldsymbol{\sigma}_f = \mathbf{E}_f : \boldsymbol{\varepsilon}_f$$
$$\dot{\boldsymbol{\varepsilon}}_m = \frac{1}{2G_m}\boldsymbol{\sigma}_m^d + \frac{1}{K_m} tr(\dot{\boldsymbol{\sigma}}_m)\mathbf{1} + \frac{1}{2\eta}\boldsymbol{\sigma}_m^d = \mathbf{E}_m^{-1} : \dot{\boldsymbol{\sigma}}_m + \mathbf{C} : \boldsymbol{\sigma}_m \qquad (11^{a,b})$$

where the subscripts *m* and *f* respectively denote matrix and fibre; $\boldsymbol{\sigma}$ and $\boldsymbol{\varepsilon}$ are the stress and linear strain tensor, respectively; **E**, **C** and **1** represent the fourth order elasticity, creep and unit tensors, respectively; *K* is the bulk modulus and *G* the shear modulus, η represents the viscosity and superscript *d* denotes the deviatoric part.

The longitudinal and transverse behaviour of the ply are described with combinations of the Maxwell element and elastic spring, assuming equal strains in the fibre direction and equal stresses in the transverse direction, see figure 5.

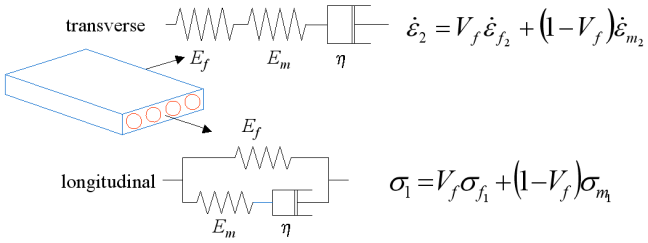

figure 5 Schematical representation of the constitutive behaviour of a UD ply

The constitutive behaviour of the ply is finally described by a matrix-vector formulation of a system of ordinary differential equations:

$$\{\dot{\sigma}\} = -[E]\cdot[C]\cdot\{\sigma\} + [E]\cdot\{\dot{\varepsilon}\} - [E]\cdot[R]\cdot\{\varepsilon\} \qquad (12)$$

where [*E*], [*C*] and [*R*] represent the orthotropic stiffness matrix, a non-symmetric creep matrix and a retardation matrix, see [9] for more details. In this model, thermorheological simplicity is assumed, i.e. the relaxation times change as a function of the temperature and cure conversion, and the elastic moduli remain constant. Equations (12) are solved analytically for a constant strain rate [10] to obtain a time-discreet relation between incremental stress, initial stress and strain at the start of a timestep and strain increment, which can be used in FE calculations:

$$\{\Delta\sigma\} = -[E^*]\cdot[C^*]\cdot\{\sigma^0\} + [E^*]\cdot\{\Delta\varepsilon\} - [E^*]\cdot[R^*]\cdot\{\varepsilon^0\} \qquad (13)$$

where [E^*], [C^*] and [R^*] respectively are the time-integrated stiffness, creep and retardation matrix depending on the elastic properties and the viscosity. The incremental strain vector contains the mechanical strain as well as the thermal and chemical strain, similar to equation (8). The stress relation discretised according to (13) shows good stability properties for larger timesteps in contrast to a forward Euler discretisation.

Chemorheology
The viscosity of the resin determines the viscoelastic behaviour of the composite. When the viscosity is low, the relaxation times are small resulting in the relaxation of mainly the transverse stresses. On the other hand, when the viscosity becomes infinite, the creep and retardation matrix become zero leading to elastic material behaviour. The viscosity can be measured up to the

vitrification point. A common relation [11] describing the viscosity as a function of temperature and cure conversion is used here:

$$\eta(T,\varphi)=\eta_0 \exp\left(\frac{U_{act}}{RT}+k_v\varphi^{m_v}\right) \tag{14}$$

where T is the temperature, φ the degree of cure, η_0 a reference viscosity, U_{act} the activation energy, R the universal gas constant and k_v and m_v are constants fitted on rheometer measurements. The cure kinetics, fitted on differential scanning calometry (DSC) measurements, are described with a universal relation:

$$\dot{\varphi}=\dot{\varphi}_{ac}+\dot{\varphi}_d=(k_1+k_2\varphi)(1-\varphi)(b-\varphi)+k_3(1-\varphi)^{m_c} \tag{15}$$

where b is a curing constant as well as k_i which are defined in terms of other constants a_i and E_i as

$$k_i=a_i \exp\left(-\frac{E_i}{RT}\right) \tag{16}$$

The first part of (15) represents an autocatalytic model for low degree of cure, while the second part describes the higher degree of cure, which is diffusion controlled.

Implementation

The viscoelastic material model, viscosity model and cure kinetics, readily available in the implicit FE package DiekA [12], were extended. The unsymmetrical crossply was meshed using generalised plane strain elements having four degrees of freedom (DOF's) on each node: two displacements u_x and u_y, the temperature T and the strain ε_z. As a first approach, the curing of the laminate was simulated excluding thermal and mechanical interaction with the tool and the environment. The temperature DOF was prescribed equally on all nodes, following the curing temperature as shown in figure 1. The internal heat generated by the exothermic polymerisation reaction was not taken into account. The laminate was fully constrained in-plane, thereby neglecting effects caused by thermal expansion and contraction of the tool. The autoclave pressure, being small compared to the internal stresses, was omitted. The chemical shrinkage was assumed to be proportional to the degree of cure.The input parameters needed for the cure kinetics and viscosity equation are listed in table 2.

Property	unit	Property	unit	Property	unit
η_0	7.725 Pa·s	a_1	0.996 s^{-1}	E_1	$3.77\cdot10^4$ J/mol
U_{act}	4.690 kJ/mol	a_2	$3.05\cdot10^3$ s^{-1}	E_2	$5.27\cdot10^4$ J/mol
R	8.314 J/(mol K)	a_3	$2.28\cdot10^{20}$ s^{-1}	E_3	$2.22\cdot10^5$ J/mol
k_v	75.0	b	0.95		
m_v	2.24	m_v	1.12		

table 2. Cure and viscosity parmeters for 8552 epoxy resin

Results

Figure 6 depicts the degree of cure and viscosity of the 8552 resin calculated with equations (15) and (14), respectivily. The viscosity decreases rapidly as the resin is heated up to the curing temperature. Subsequently, the cure conversion causes a sharp increase of the viscosity after about 100 minutes. The further increase after 200 minutes due to the cooling to room temperature has no physical meaning; as discussed, the viscosity was only measured up to the vitrification point. The cure kinetics and the resulting viscosity agree reasonably with recent work by Ng et al. [13].

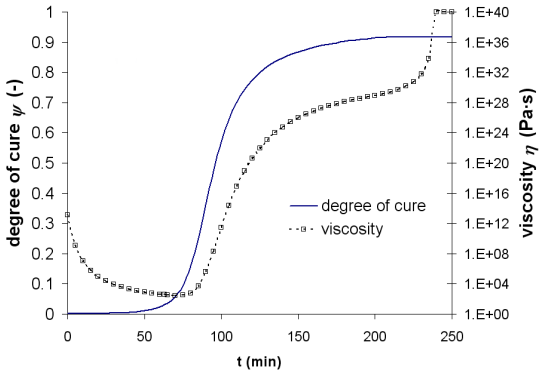

figure 6. Cure conversion and viscosity calculated for the temperature profile of figure 1

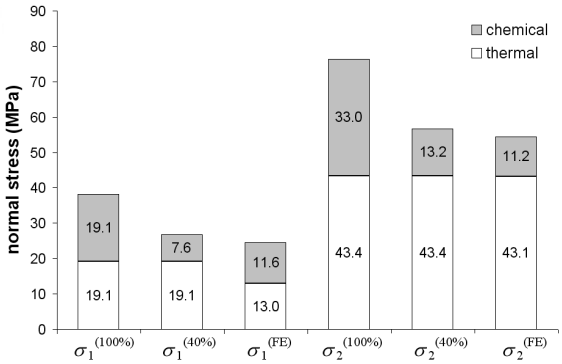

figure 7. Numerical results compared to analytical results

The resulting normal stresses in the global *x*-direction before release are compared to the analytically derived stresses in figure 7. Both the thermal and chemical part of the transverse stress $\sigma_2^{(FE)}$ calculated with the viscoelastic model agree very well with the stress $\sigma_2^{(40\%)}$ which complies with the measured curvature. Therefore, the curvature calculated with $\sigma_1^{(FE)}$ and $\sigma_2^{(FE)}$ as κ_x = 3.04 m^{-1} shows good agreement with the measured curvature of 3.1 m^{-1}. The differences in the thermal and chemical parts of the longitudinal stresses $\sigma_1^{(FE)}$ and $\sigma_1^{(40\%)}$ are larger. However, the total stresses agree within 8%: 24.6 vs. 26.7 MPa. An explanation follows from figures 8 and 9, which show the development of the longitudinal and transverse stress.

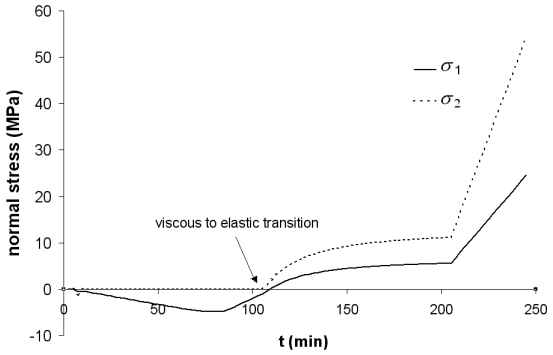

figure 8. Stress in the global x-direction of the 0° and 90° ply, respectively σ_1 and σ_2.

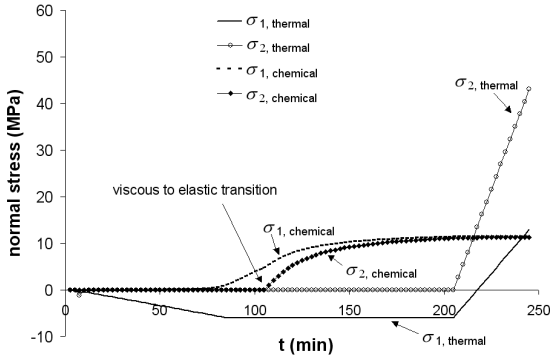

figure 9. The stresses split into a thermal and a chemical part

Figures 8 and 9 demonstrate that the transverse stress is equal to zero up to 105 minutes, and subsequently starts building up. This stress is caused by chemical shrinkage as can be seen in figure 9 where the longitudinal and transverse stresses are split into a thermally and chemically induced part. The transverse material behaviour is dominated by the resin, see figure 5. Obviously, the resin is viscous up to 105 minutes, relaxing all transverse stress.

The cooling down takes place when the resin is completely elastic. The longitudinal thermal stress before release at room temperature is smaller for the FE model than for the analytical model due to the compressive stresses induced during heating up. The chemically induced longitudinal stress is larger, though; more than the estimated 40% of the total chemical shrinkage causes stress as the fibre stress cannot relax. This is the result of an inconsistency in the treatment of the chemical strain. Subjecting the parallel configuration of the longitudinal direction (see figure 5) to a chemical strain according to equation (9) allows for the buildup of fibre stress, even when the matrix stress relaxes completely.

Viscous to elastic transition

Comparing the viscoelastic model with an elastic calculation performed with the FE model by setting the viscosity of the resin to $1 \cdot 10^{40}$ showed that the transition at 105 minutes is instant from viscous to completely elastic. In the spring-damper model that is applied here, and often in general visco-elasticity, a common measure for the response of a material in a mechanical process is the Deborah number:

$$De = \frac{t_p}{t_{rel}} \tag{17}$$

where t_p is the process time and t_{rel} is the relaxation time. The latter is a time constant defined by

$$t_{rel} = \frac{\eta}{E_m} \tag{18}$$

The following classification is made:

$De << 1$	$\rightarrow$	elastic response
$De >> 1$	$\rightarrow$	viscous response
$De \approx 1$	$\rightarrow$	visco-elastic response

Here, $De = 1$ at 105 minutes using a timestep of 150 s. Solving a one-dimensional relaxation test with a Maxwell element shows that the classification above can be specified as:

$De < 0.1$	$\rightarrow$	elastic response
$De > 10$	$\rightarrow$	viscous response

of which becomes clear that the transition from viscous to elastic material behaviour takes place in a single time increment. Figure 6 shows that the degree of cure at the transition point is 60%, which corresponds with the adjustment of the chemical strain to 40% of the total chemical strain in the analytical model.

5 CONCLUSIONS

The curvature of fully cured unsymmetric [0/90] laminates made from AS4/8552 UD tape was measured. This curvature was demonstrated to be a good measure for the transverse stress being present in the 90° ply before the laminate is released from the tool. Firstly, the transverse stress was predicted using a analytical, linear elastic approach including thermal shrinkage and contraction of the resin due to crosslinking. It showed that the model gives sensible results when the chemical shrinkage is corrected for shrinkage occuring before the vitrification point. Secondly, the residual stress state before release from the tool was calculated numerically applying a viscoelastic material model. The model incorporates the cure conversion and the resulting change in viscosity, both fitted on experimentally obtained data. It showed that the curvature related to the computed stress state agrees very well with the measured curvature. The correction of the chemical shrinkage in the analytical approach was confirmed by the numerical model.

The investigations show that the non-symmetric crossply experiment is an accurate method to determine the transverse residual stresses present in the laminate before demoulding. It thus serves as a critical benchmark for the complex material modelling of internal stress generation during composite moulding and the subsequent post-mould component distortions. Secondly, the analytical model provides a quick estimate for the stress-inducing part of the strain caused by the

polymerisation of the resin. This estimate can subsequently be applied in linear elastic finite element simulations of the cooling stage in the forming of complex product geometries.

ACKNOWLEDGEMENTS

The authors would like to acknowledge the European Union for the funding of the Precimould project, EU grant BE97-4351. The project partners are gratefully acknowledged for the technical support.

REFERENCES

[1] S. Wijskamp and R. Akkerman, Residual stress measurements, Precimould report PREC-UOT-WP7-REP-133, 2001.
[2] M.W. Hyer, Some observations on the cured shape of thin unsymmetric laminates, *Journal of Composite Materials*, **15**, 1981, 175-194.
[3] W. Hufenbach, M. Gude, Analysis and optimisation of multistable composites under residual stresses, *Composite Structures*, **55**, 2002 319-327.
[4] M. Gigliotti, M.R. Wisnom, K.D. Potter, Development of curvature during curing of AS4/8552 [0/90] unsymmetric composite plates, *Composites Science and Technology*, **63**, 2003, 187-197.
[5] P.C. Powell, *Engineering with fibre-polymer laminates*, Chapman and Hall (London), 1994.
[6] R.A. Shapery, Thermal expansion coefficients of composite materials based on energy principles, *Journal of Composite Materials*, **2**, 1968, 380.
[7] M.P.I.M. Eijpe, *A modified layer removal method for determination of residual stresses in polymeric composites*, Ph.D.-thesis, University of Twente, 1997.
[8] A. Johnston, R. Vaziri and A. Pousartip, A plane strain model for process-induced deformation of laminated composite structures, *Journal of Composite Materials*, **35**, 2001, 1435-1469.
[9] H.W. Wiersma, L.J.B. Peeters and R. Akkerman, Prediction of springforward in continuous-fibre/polymer L-shaped parts, *Composites Part A*, **29**A, 1998, 1333-1342.
[10] R. Akkerman, *Euler-Lagrange simulations of nonisothermal visoelastic flows*, Ph.D.-thesis, University of Twente, 1993.
[11] M.V. Bruschke and S.G. Advani, A numerical approach to model the non-isothermal viscous flow through fibrous media with free surfaces, *International Journal of Solids and Structures*, **19**, 1994, 575.
[12] J. Huétink, P.T. Vreede and J. van der Lugt, Progress in mixed Eulerian-Lagrangian finite element simulation of forming processes, *International Journal for Numerical Methods in Engineering*, **30**, 1990, 1441.
[13] S.J. Ng, R. Boswell, S.J. Claus, F. Arnold and A. Vizzini, Degree of cure, heat of reaction and viscosity of 8552 and 977-3 HM epoxy resins, *Journal of Advanced Materials*, 2002, 33-37.